Observations of the Ag(3x1) phase on Ge(111)

Running title: Observations of Ag(3x1) Phase on Ge(111)

Running Authors: Mullet, Rosen, and Chiang

Cory H. Mullet, ¹ Anna L. Rosen, ² and Shirley Chiang³

Department of Physics University of California, Davis

1 Shields Avenue

Davis, California 95616-5270, USA

Abstract

Low energy electron diffraction (LEED) and low energy electron microscopy (LEEM) were used

to study the (3x1) phase of Ag on Ge(111) for temperatures less than 540°C. This phase was

observed when depositing 0.05 to 0.1 ML Ag at 370°C. The $(\sqrt{3} \times \sqrt{3})R30^{\circ}$ phase formed when

depositing 0.3ML Ag at 170°C and then annealing to 200-360°C resulted in a non-reversible phase

transition to [(4x4) + (3x1)] phases at 360°C. The $\sqrt{3}$ phase appears to be metastable for

temperatures <250°C since subsequent cooling did not cause it to reappear. These experimental

observations suggest modifications to a published phase diagram for Ag/Ge(111).

Keywords: Ag; Germanium; (3x1) Phase; Low Energy Electron Microscopy; Low Energy

Electron Diffraction

¹ Present address: Intel Corporation, Hillsboro, OR, 97124, USA

² Present address: Center for Astrophysics, Harvard and Smithsonian, 60 Garden St., Cambridge,

MA 02138, USA.

³ Corresponding author: chiang@physics.ucdavis.edu

1

I. INTRODUCTION

Metals on semiconductors have been studied for decades as prototypical systems for fundamental surface science studies. These systems include Ag, Au, Sn, Pb, and Ni adsorbed onto elemental semiconductor surfaces, including both Si(111) and Ge(111).¹⁻¹¹ In addition, better understanding of these systems could improve the formation of metal contacts for semiconductor devices, especially as device linewidths continue to shrink down towards the atomic scale.

For coverage less than 1.0 monolayer (ML), Ag on Ge(111) has a particularly complex phase diagram, as shown in Fig. 1, which published by Grozea et al.¹² For submonolayer Ag coverages on Ge(111), eight different phases have been reported: (4x4), $(\sqrt{3}x\sqrt{3})R30^{\circ}$, $(3x1)^{2,13}$, (1x1), (5x1), (5x1), $(12\sqrt{3}x12\sqrt{3})R30^{\circ}$, (6x6), (6

Clean Ge(111) has a well-known c(2x8) reconstruction, but it undergoes a high temperature phase transition at 300°C to an incommensurate structure. In a LEED study, Phaneuf and Webb¹⁸ described this structure as either three orientations of (2x1) structures with quasiperiodic antiphase walls or a (2x2) reconstruction modulated by a honeycomb arrangement of intersecting antiphase walls. When Ag is deposited onto the Ge(111) surface, the two dominant phases observed are the (4x4) and ($\sqrt{3}$ x $\sqrt{3}$)R30° (abbreviated here as $\sqrt{3}$), and both have accepted structures from the literature. The (4x4) structure is a missing top layer reconstruction with Ag surface coverage of 0.375 ML.^{2, 14, 19} The $\sqrt{3}$ phase has the "honeycomb chained trimer" reconstruction with a Ag surface coverage of 1.00 ML,^{3, 14, 17} and its structure is similar to the $\sqrt{3}$ reconstruction of Ag on Si(111).^{4, 20}

This paper describes primarily LEED and LEEM observations of the (3x1) phase of Ag on Ge(111) for temperatures less than 540°C, elucidating the complicated phase diagram of this metal on semiconductor system. The structure of the (3x1) phase has been determined as the "honeycomb chain channel" reconstruction, which has a Ag surface coverage of ~1/3 monolayer $(ML)^{21}$ and is similar to the Ag (3x1) structure on Si(111).²² Only one previous study observed large regions of the Ag (3x1) phase on Ge(111),²¹ whereas other studies reported observations of the (3x1) phase as small domains bordering regions of (4x4) structure and clean Ge.^{2, 14, 23} Giacomo²⁴ did not observe the (3x1) phase at all.

The phase diagram in Fig. 1 shows that the (3x1) phase primarily occurs in the temperature range between 350 and 450°C. It occurs alone for Ag coverage between 0.1 and 0.3ML Ag, and coexists with the Ge(111) c(2x8) structure, the (4x4) Ag structure, and the $\sqrt{3}$ Ag structure in nearby regions of the phase diagram. In addition to corroborating most of the (3x1) sections of Grozea's phase diagram, we also observed the (3x1) phase in additional regions of the phase diagram, as described in detail in Sect. III. Furthermore, our measurements suggest that the $\sqrt{3}$ phase, which reproducibly occurs for Ag growth on substrates between 150 and 200°C, is metastable.

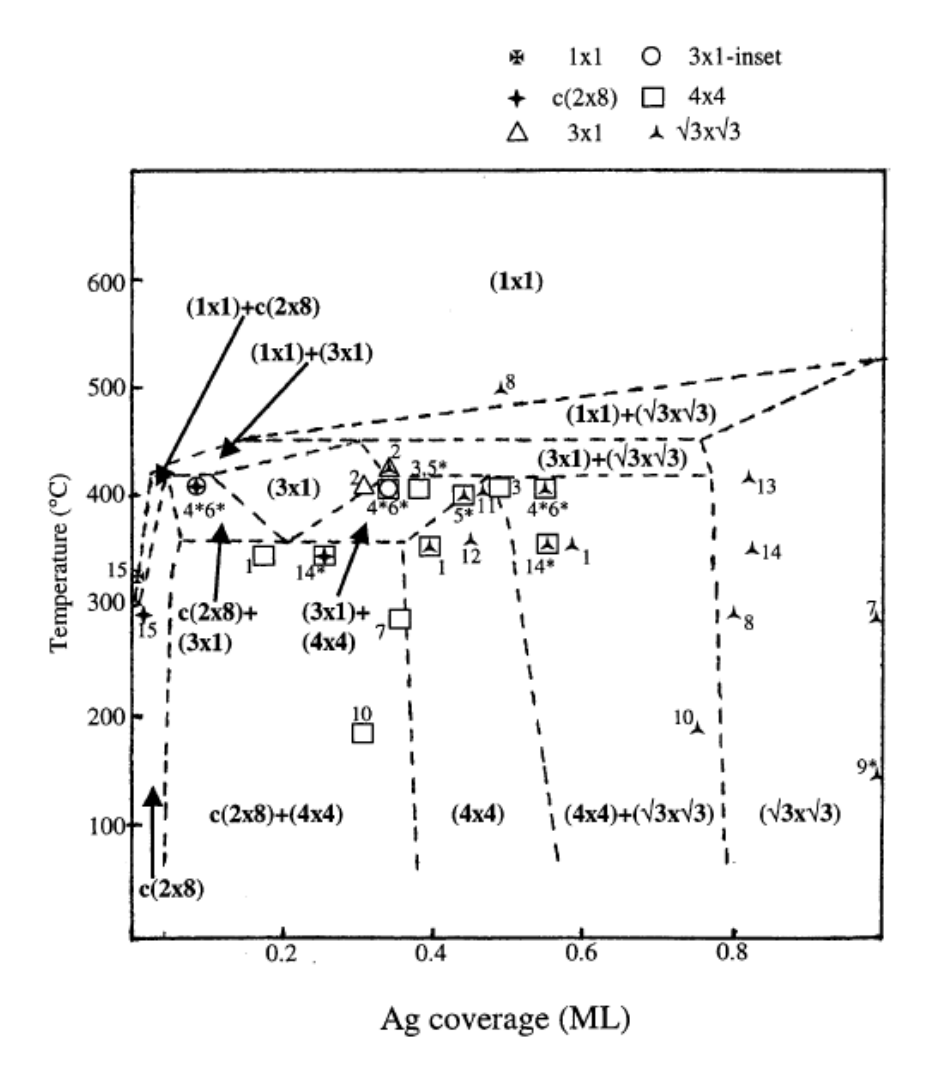


Fig. 1. Ag/Ge(111) surface phase diagram proposed by Grozea et al. in Ref. 12. Reprinted from Surface Science, Vol. 461, D. Grozea, E. Bengu, and L. D. Marks, Surface phase diagrams for the Ag–Ge(111) and Au–Si(111) systems, pages 23-30, Copyright (2000), with permission of Elsevier.

II. EXPERIMENTAL

Measurements were carried out in a ultrahigh vacuum (UHV) system consisting of connected chambers housing three major commercial instruments: low energy electron

microscope (LEEM, Elmitec GmbH), scanning tunneling microscope (STM, Oxford Instruments), and x-ray photoemission spectrometer (XPS, Vacuum Generators).²⁵

Ge(111) samples were cut from Sb-doped Ge(111) 2-inch wafers purchased from MTI Crystal, with resistivity \sim 0.25 Ω -cm and polished on one side within 0.5° of the (111) surface. Ge(111) crystals were cleaned in the UHV analysis chamber (base pressure 2×10^{-10} Torr) with repeated cycles of Ar⁺ bombardment (250 eV, 5 μ A) of the unheated sample for 15 minutes, followed by annealing the sample between 800°C and 830°C for 10 minutes (30 minutes for the last anneal before imaging in LEEM or STM). Samples were sputtered and annealed until a clean c(2×8) low energy electron diffraction (LEED) pattern was obtained. Following the cleaning cycles, the sample was transferred to the LEEM chamber (base pressure 1×10⁻¹⁰ Torr) or STM chamber (base pressure 4×10⁻¹⁰ Torr). XPS was also occasionally used to verify that the sample was free from contaminants.

Sample heating was monitored by a K-type thermocouple with the junction pressed against the back of the sample. The thermocouple was calibrated with an infrared pyrometer with the emissivity set to 0.42, which was determined by calibrating the pyrometer to the melting point of an old Ge sample. The thermocouple calibration was checked by using LEED to measure the temperature for the $c(2\times8)$ to (2×1) phase transition on clean Ge(111) at 300°C.¹⁸

Direct evaporation from a resistively heated Ag wrapped tungsten filament was used to deposit Ag onto the Ge(111) sample while imaging with either LEED or LEEM. The deposition rate was calibrated in the LEEM by measuring the time for completing either the (4×4) Ag phase at 0.375 ML or the $\sqrt{3}$ phase at 1.00 ML. A range of deposition rates (0.005-1.5 ML/min) was employed depending upon the phenomena under study.

III. EXPERIMENTAL RESULTS AND DISCUSSION

A. Formation of (3x1) phase by deposition of Ag on Ge(111) at 330-370 °C

The (3x1) phase was observed to form at low coverage, before growth of the (4x4) or $\sqrt{3}$ phases. For deposition at 370°C, (3x1) was the only phase of Ag on the surface for coverage up to 0.1 ML, as evidenced by the LEED pattern in Figure 2(a). The first Ag LEED spots observed are somewhat faint, elongated spots consistent with three rotational domains of Ag (3x1), and they coexist with spots from the Ge(2x1) structure. Figure 2(b) shows the LEEM image that corresponds to the LEED pattern in Fig. 2(a). Narrow domains of (3x1) decorate the step edges and defects of this highly stepped sample. The contrast seen in this image appears to be due to phase contrast between the Ge substrate and regions having the Ag (3x1) structure, rather than due to substrate step contrast. Fig. 2(c) and (d) show the LEED pattern and LEEM image after the Ag was desorbed from the surface. Note that the step contrast on Ge(111) is very faint at voltages of 5.0-5.2 eV in Fig. 2(d), where the observed Ag (3x1) contrast is a maximum. In addition, the phase contrast between (3x1) and Ge in Fig. 2(b) is roughly the same as that between (4x4) and Ge at this imaging energy in other LEEM images, for which the (4x4) is bright and Ge is dark. From LEEM images alone, it would be difficult to distinguish between very low coverages (<0.1 ML) of (3x1) Ag and (4x4) Ag. The (3x1) LEED pattern of the surface in Fig. 2(a) verifies that the bright LEEM regions indeed correspond to the (3x1) phase.

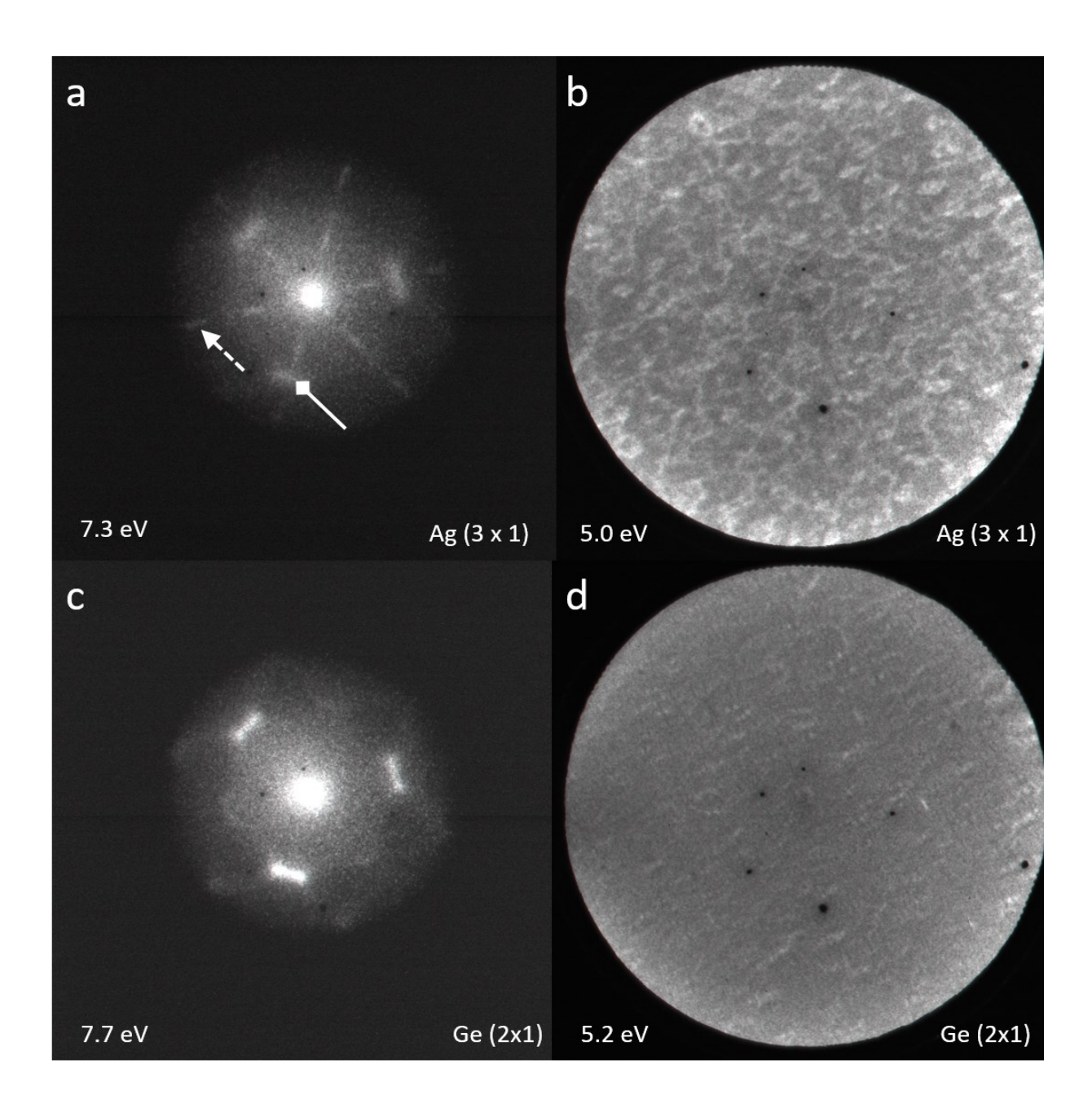


Fig. 2. LEED patterns and LEEM images before and after desorption of Ag (3x1) from Ge(111). (a) After deposition of 0.05-0.1 ML Ag at 370 °C. Ag (3x1) LEED spots (dashed arrow) coexist with Ge (2x1) LEED features (diamond head arrow), which were present before the Ag deposition. (b) After Ag deposition on Ge(111), LEEM image corresponding to the (3x1) LEED pattern in (a). Ge (dark areas) and Ag (3x1) (bright areas). FOV 5 μm. (c) Clean Ge (2x1) LEED pattern after desorption of Ag. (d) LEEM image corresponding to LEED pattern in (c), after desorption of Ag. FOV 5 μm.

Figure 3 shows LEED, LEEM, and STM measurements of the same sample, which had 0.59 ML of Ag deposited onto Ge(111) at 330 °C. LEED and LEEM imaging were performed during the Ag deposition process. At this coverage and deposition temperature, the LEED pattern in Fig. 3(a) shows strong (4x4) and $\sqrt{3}$ spots, together with weak (3x1) spots. The LEEM image in Fig. 3(b) shows primarily bright $\sqrt{3}$ and dark (4x4) structures, as the (3x1) domains are too small to resolve with LEEM. The sample was cooled to room temperature, without a significant change occurring in either the LEEM image or the LEED pattern. Then the sample was moved into the STM, where we observed the (3x1) phase as narrow regions along (4x4) Ag domains (Fig. 3(c)), similar to previous STM studies.^{2, 14, 23} The (3x1) regions often appear as small insets between (4x4) regions and small domains (<10 nm in size) of Ge(111) c(2x8) that persist at this coverage (Fig. 3(c)). The sizes of the (3x1) and (4x4) unit cells from our STM images agree with the dimensions reported in earlier studies.^{2, 14, 23}

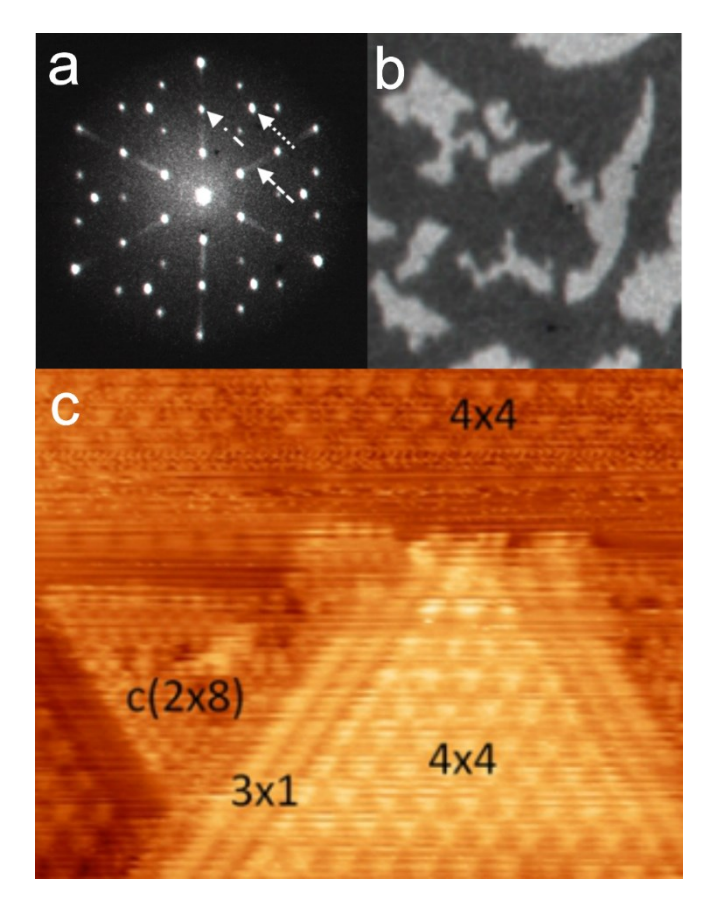


Fig 3. (color online) Ag deposited on Ge(111) at 330 °C while imaging with LEEM and LEED, followed by STM measurements at room temperature. $\Theta = 0.59$ ML. (a) LEED picture showing $\sqrt{3}$, (4x4), and faint (3x1) spots. Several spots are indicated with arrows: $\sqrt{3}$ (dotted arrow), (3x1) (dashed arrow), and the [0, $\sqrt{2}$] (4x4) spot (dot-dash arrow). (b) LEEM image showing regions with $\sqrt{3}$ (bright) and (4x4) (dark) structures. FOV = 2 μ m, E = 4.0 eV. E = 8.1 eV. (c) Empty state STM image. Regions of (4x4), c(2x8), and (3x1) Ag indicated. Sample bias = +1.0 V, tunneling current = 0.5 nA. 19 nm x 15 nm.

For Ag deposition onto a Ge(111) sample held at 370 °C, (3x1) was the only phase of Ag on the surface for coverage up to 0.1 ML. As additional Ag is deposited, Ag (3x1) spots intensify as the (4x4) and then $\sqrt{3}$ phases form. For about 0.4ML Ag coverage, the LEED pattern looks similar to that in Fig. 3(a), for which all three Ag phases coexist on the surface. As the coverage approaches 1.0 ML, the (4x4) and (3x1) phases extinguish approximately simultaneously, leaving

only the $\sqrt{3}$ phase on the surface. These observations match the phases expected at this temperature as a function of coverage from the phase diagram in Fig. 1.

B. Deposition of Ag on Ge(111) at 170°C and $\sqrt{3} \rightarrow [(4x4) + (3x1)]$ phase transformation at 360 °C

The (3x1) phase was also observed, along with (4x4) and $\sqrt{3}$ phases, when the surface was prepared by depositing Ag at lower temperature and then annealing. When Ag is deposited at ~150-220 °C, the $\sqrt{3}$ phase grows before the (4x4), as observed previously by Giacomo.²⁴ LEED and LEEM images of 0.3 ML of Ag $\sqrt{3}$ growth at 170 °C are shown in Figure 4. Ag $\sqrt{3}$ growth in this low temperature regime is characterized by small domain sizes.²⁴ The LEEM image in Fig. 4(d) shows Ag $\sqrt{3}$ island sizes of ~100 nm in diameter.

Annealing the $\sqrt{3}$ surface in Fig. 4(d) results in the transformation of the $\sqrt{3}$ phase to (3x1) and (4x4) phases, as seen in the LEED images of Fig. 5. As the temperature is raised to 290 °C, definite (3x1) LEED spots and weak (4x4) spots indicate the formation of those phases (Fig. 5(b)) from the $\sqrt{3}$ Ag phase previously on the surface (Fig. 5(a)). The (3x1) and (4x4) LEED spots intensify, and the $\sqrt{3}$ spots become somewhat dimmer as the temperature is increased, up to 360°C where the $\sqrt{3}$ spots vanish, leaving a strong [(4x4) + (3x1)] LEED pattern (Fig. 5d). The $\sqrt{3} \Rightarrow$ [(4x4) + (3x1)] transformation at 360 °C is quite sudden (Fig. 5(cd)) compared to the gradual $\sqrt{3} \Rightarrow$ [(4x4) + (3x1)] transformation that takes place between 200-350 °C (Fig. 5(abc)). While our observation of the (3x1) phase at $\Theta = 0.3$ ML, T = 290-350°C conflicts with the surface phase diagram proposed by Grozea et al. ¹² (Fig. 1), the sudden completion of the transformation at 350-360 °C supports their placement of the lower bound of the (3x1) phase at 350°C.

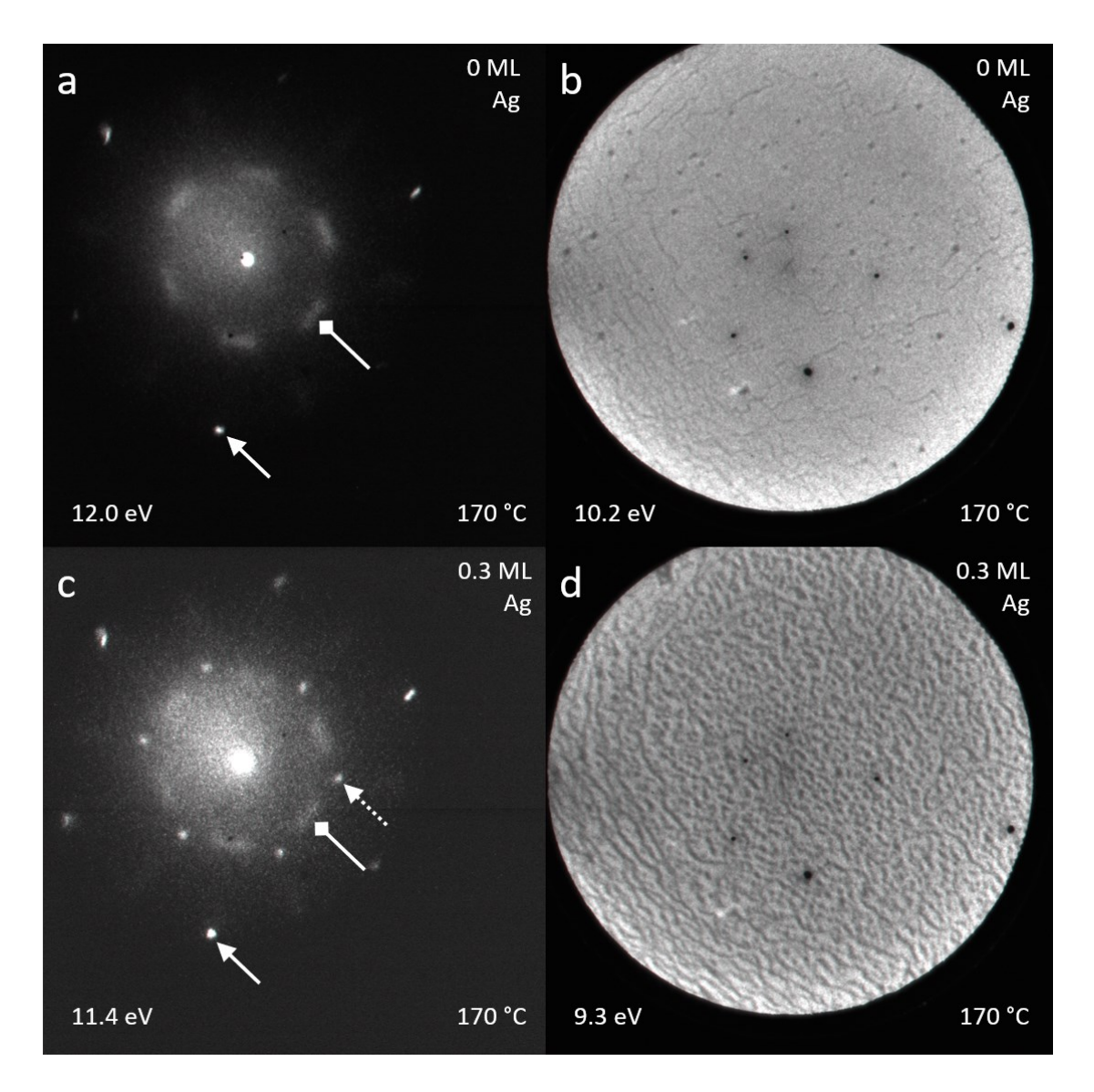


Fig. 4. LEED patterns and LEEM images of the deposition of 0.3 ML Ag onto Ge(111) at 170 °C. Diamond head arrows and dotted arrows point to the Ge(2 x 1) and $\sqrt{3}$ Ag LEED spots, respectively. Solid arrows point to first-order Ge(111) LEED spots. (a) Clean Ge(111) LEED image. First order LEED spots (solid arrow) as well as Ge(2x1) features (diamond head arrow) are visible at this energy. (b) Clean Ge(111) LEEM image. 5 μ m FOV. The sample surface has a high step density, especially on the periphery of the field of view. Small dark circles are defects in the microchannel plate, and larger dark spots are substrate defects. (c) LEED image shows additional $\sqrt{3}$ Ag spots (dotted arrow) after deposition of 0.3 ML Ag. (d) LEEM image corresponding to LEED image in (c), after deposition of 0.3 ML Ag. Dark areas correspond to $\sqrt{3}$ Ag and bright areas to Ge regions. 5 μ m FOV.

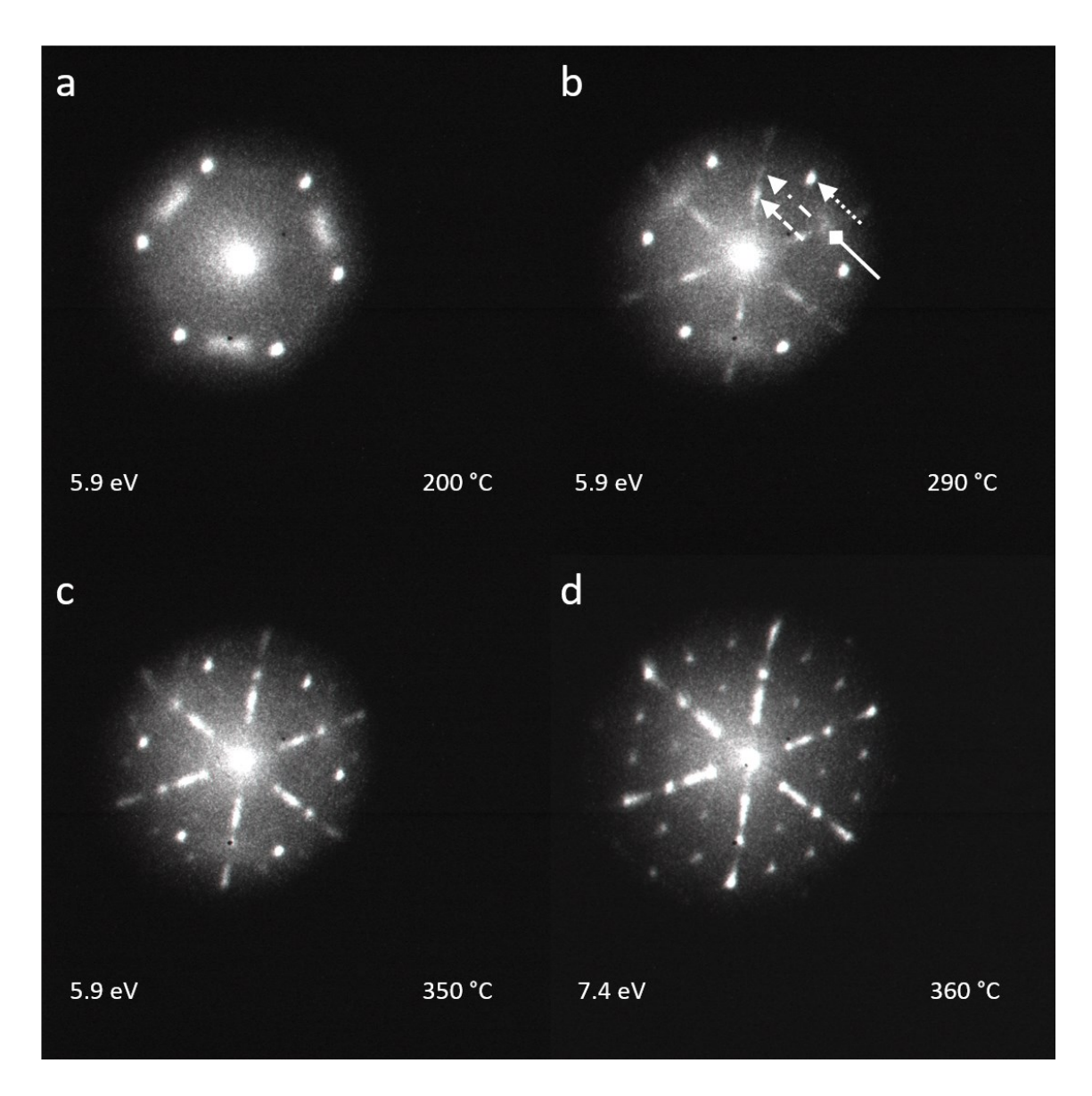


Fig. 5. After dosing 0.3ML Ag on Ge(111), LEED images during heating to indicated temperatures. See Fig. 4 for LEED/LEEM of this sample after initial deposition. Different arrows in (b) identify LEED spots: Ge(2 x 1) (diamond head arrow), Ag (3x1) (dashed arrow), Ag (4x4) (dot-dash arrow), and Ag $\sqrt{3}$ (dotted arrow). (a) $\sqrt{3}$ Ag and (2 x 1) Ge. (b) Four coexisting structures are evident: $\sqrt{3}$ Ag, (2 x 1) Ge, (3x1) Ag, and (4x4) Ag (faint). (c) Spot intensities have changed for the 4 coexisting structures: $\sqrt{3}$ Ag, (2 x 1) Ge (faint), (3x1) Ag, (4x4) Ag. (d) Only (3x1) Ag and (4x4) Ag spots remain.

The $\sqrt{3} \rightarrow [(4x4) + (3x1)]$ transformation that occurs between 200 and 360 °C at 0.3 ML coverage is not reversible. When the sample is cooled below 350 °C, the [(4x4) + (3x1)] LEED pattern does not change (Fig. 6(b)). This observation was repeated for all similar experiments carried out with $\Theta < 0.375$ ML; once the (4x4) and (3x1) phases were present on the surface, the sample could be cooled down all the way to room temperature without a noticeable change in either the LEEM images or LEED patterns. The domains of (3x1) and (4x4) as viewed in LEEM are as small or smaller than the domains of $\sqrt{3}$ that formed during deposition (\leq 100 nm in diameter) (Fig. 6(a)). Surfaces of the (4x4) and (3x1) phases created by deposition at low temperature and then annealing to high temperature all showed domain sizes smaller than those that would have resulted had Ag been deposited directly onto samples held at the annealing temperature.

The non-reversible nature of the $\sqrt{3} \rightarrow [(4x4) + (3x1)]$ transformation from 200-360 °C supports Grozea et al.'s designation of the (4x4) phase as the equilibrium Ag phase(s) for $\Theta < 0.375$ ML, T < 350 °C (Fig. 1).¹² Our results, however, indicate that the (3x1) phase should also be added to this region of the phase diagram. In addition, we deduce that the $\sqrt{3}$ phase, which was repeatedly observed in this study (Figs. 4 and 7(a)) and also by Giacomo²⁴ for Ag deposition onto samples with temperatures ~120-220 °C, should therefore be interpreted as a nonequilibrium phase.

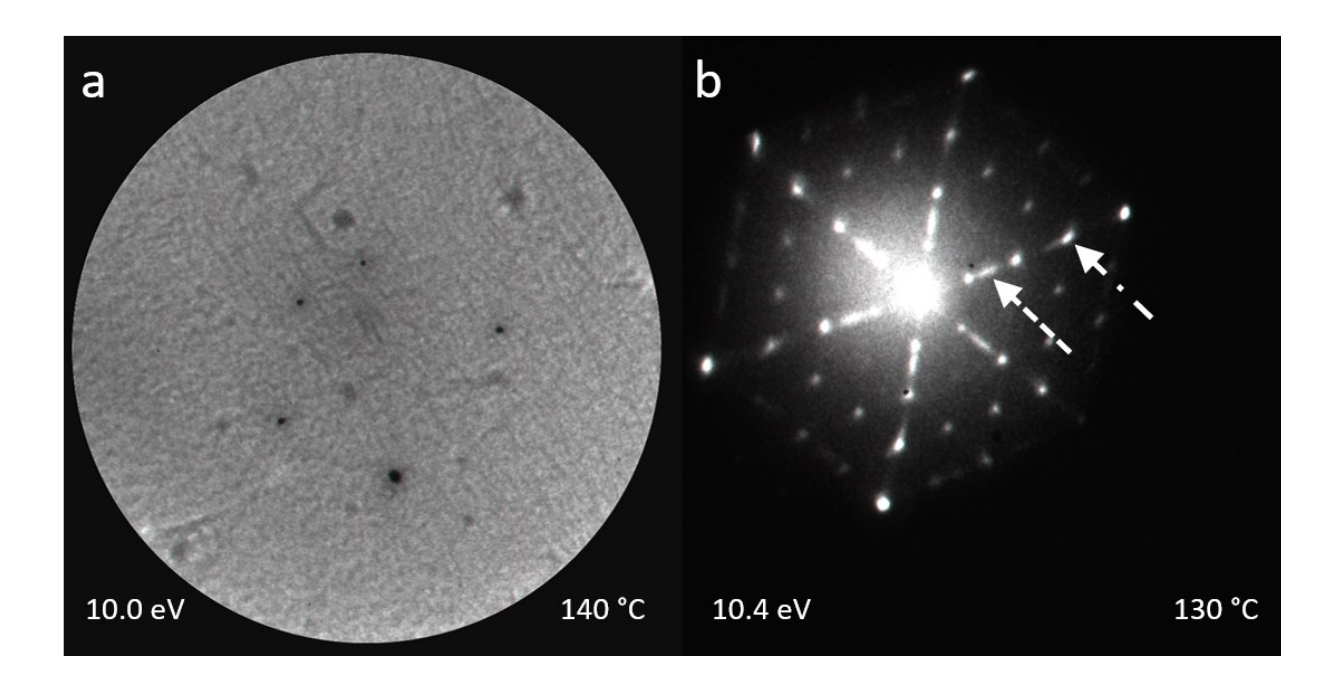


Fig. 6. Upon cooling the sample shown in Fig. 5(d), the LEED pattern does not change significantly. The Ag $\sqrt{3}$ phase does not return after cooling. (a) 4 μ m LEEM images of Ge(111) (bright areas) covered with small (\leq 100 nm) domains of [(4x4) + (3x1)] (dark areas). It is not possible to distinguish between the (4x4) and (3x1) phases. The largest dark spots in the image are substrate defects. (b) LEED pattern of the surface in (a), showing (4x4) (dot-dash arrow) and (3x1) (dashed arrow) spots.

Now we briefly compare this low temperature phase transition to the one which occurs at high temperature (\sim 560°C, just below the 575°C Ag desorption temperature) that we described in an earlier paper.²⁶ In that case, the reversible phase transition $[(3x1)+(4x4)] \leftarrow \rightarrow (3x1)$ was observed with LEEM and LEED for coverages less than 0.375 ML. That study also found that the (3x1) phase is energetically preferred over the (4x4) phase for temperatures above 575°C, as it persists above the desorption temperature longer than the (4x4) phase.

C. Deposition of 0.5ML Ag on Ge(111) at 220°C, followed by annealing to 580°C

Figure 7 shows LEED patterns from 0.5 ML of $\sqrt{3}$ Ag gradually heated to the desorption temperature. After the initial deposition of 0.5 ML at 220 °C, Figure 7(a) shows the $\sqrt{3}$ LEED pattern. As the temperature is raised beyond 250 °C, the $\sqrt{3}$ phase transforms to (3x1) and (4x4) phases (Fig. 7(b)), similar to the transformation observed at 0.3 ML coverage (Fig. 5). The difference between the two coverages is first observed at 410-480 °C, where the (4x4) LEED spots disappear for the 0.5 ML coverage (Fig. 7(c)), whereas they persist up to the desorption temperature for 0.3 ML coverage. At the higher 0.5 ML coverage, most (3x1) LEED spots are extinguished at 540 °C (Fig. 7(d)), whereas at the lower 0.3 ML coverage, the (3x1) phase persists up to and beyond the desorption temperature. In summary, at low coverage (0.3 ML) and high temperatures (480-580 °C), the less dense (3x1) (1/3 ML/layer) $^{19, 22}$ and (4x4) (3/8 ML/layer) phases are favored over the more dense (1.0 ML/layer) $\sqrt{3}$ phase. At a higher coverage (e.g., 0.5 ML, which is greater than the completion coverages of the (3x1) and (4x4) phases), the $\sqrt{3}$ phase is favored in this high temperature (480-580 °C) range.

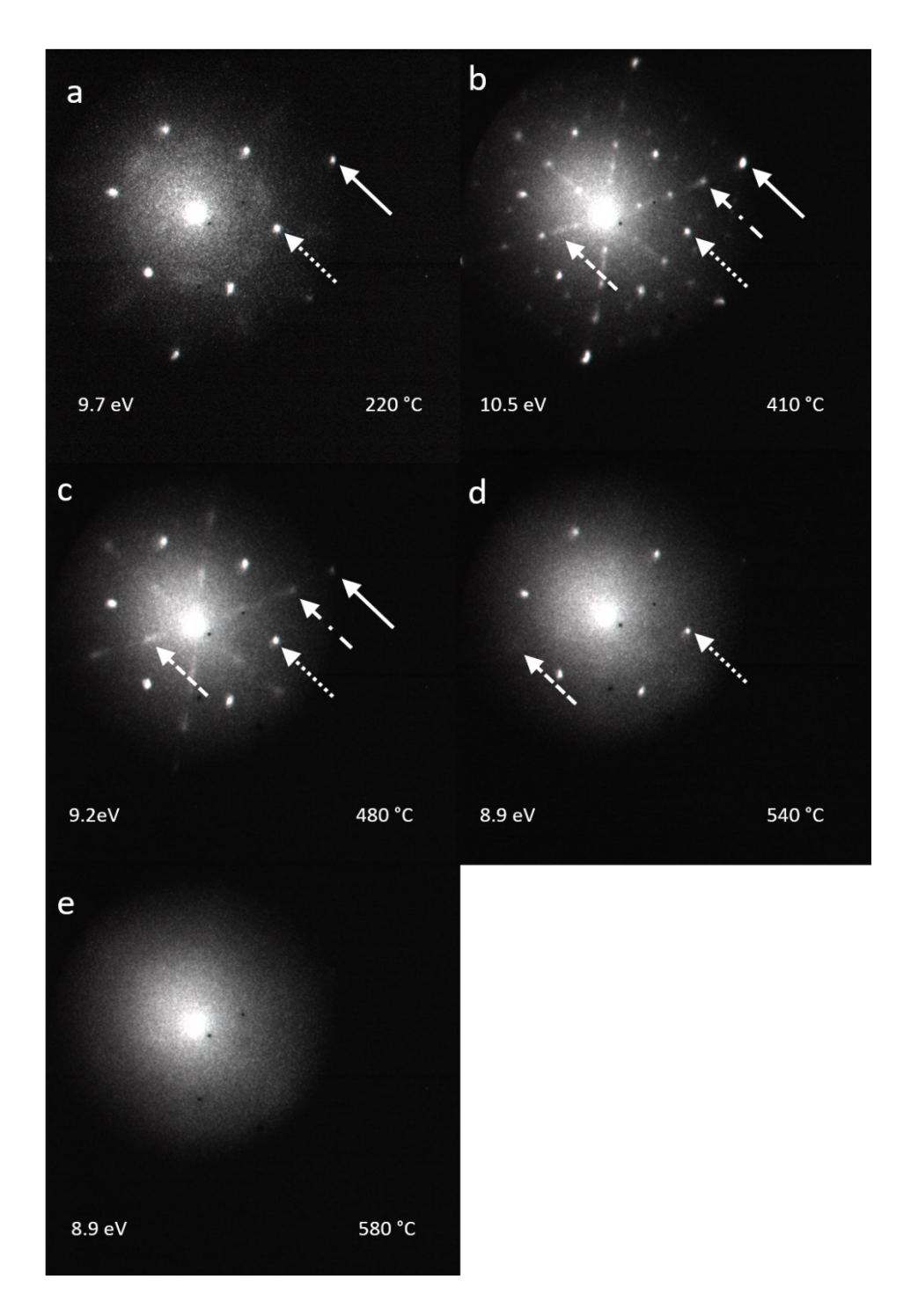


Fig. 7. Heating 0.5 ML Ag in LEED. Arrows identify LEED spots: Ge (1 x 1), solid arrow; Ag $\sqrt{3}$, dotted arrow; Ag (3x1), dashed arrow; Ag (4x4), dot-dash arrow. (a) After deposition of 0.5 ML Ag at 220 °C, $\sqrt{3}$ Ag. (b) $\sqrt{3}$ Ag + (4x4) Ag + (3x1) Ag (faint). (c) $\sqrt{3}$ Ag + (3x1) Ag (very faint). (d) $\sqrt{3}$ Ag + (3x1) Ag (very faint). (e) Clean Ge after Ag desorption.

D. Confirmations and modifications to Ag/Ge(111) phase diagram

One significant modification to the phase diagram in Fig. 1 indicated by the data presented here is the extension of the (3x1) phase, and possibly the (4x4) phase, to higher temperatures. Grozea et al. 12 has (4x4) and (3x1) extinguished by 410-450 °C at all submonolayer coverages, whereas we observed the (3x1) phase up to the Ag desorption temperature at 0.3 ML 26, and up to 540 °C at coverages of 0.5 ML (Fig. 7). The (4x4) phase was also observed up to the desorption temperature when 0.3 ML was annealed. 26 The LEED and LEEM observations presented here indicate that the upper limits of the (3x1) and (4x4) low coverage phases should be increased 50-100°C above the temperatures given in the phase diagram of Fig. 1.

Another significant modification to Fig. 1 is at low temperatures. We observed the presence of the (3x1) phase coexisting with the (4x4) phase, at coverages greater than 0.05-0.1 ML, all the way down to room temperature. Fig. 1 instead had a lower threshold of 350°C for the (3x1) phase. While the (3x1) and (4x4) phases were observed at lower temperatures (30-220 °C), they were obtained either by annealing the Ag-deposited surface to >250 °C or by deposition at $T \ge 250$ °C, followed by cooling below 250 °C. Deposition at ~100-220 °C resulted in growth of the $\sqrt{3}$ phase (e.g., Figs. 4, 7(a)), without (4x4) or (3x1), in agreement with the observations of Giacomo. The stability of the (4x4) and (3x1) phases upon cooling through 250 °C, however, leads us to conclude that they are the equilibrium phases below 250 °C, even though the initial growth phase for deposition in this temperature regime is $\sqrt{3}$. As already stated, we conclude that the $\sqrt{3}$ phase is metastable in this region of the phase diagram.

The inclusion of a region in the phase diagram that is composed exclusively of $[(3x1) + \sqrt{3}]$ within a narrow band of temperatures above 400 °C and at coverages between roughly 0.4-0.8 ML (Fig. 1) is confirmed by our LEEM and LEED observation of these phases at 0.5 ML

coverage (Fig. 7(c)). The non-reversible phase transformation $\sqrt{3} + (4x4) + (3x1) \Rightarrow [(3x1) + \sqrt{3}]$ at 410-480 °C at 0.5 ML (Fig. 7(bc)), closely corresponds to Fig. 1 in this region. In addition, the region of Fig. 1 with $[(1 \times 1) + \sqrt{3}]$ immediately above the $[(3x1) + \sqrt{3}]$ region is confirmed by Fig. 7(d). The confirmation of these two regions of the phase diagram in Fig. 1 is particularly interesting because the literature shows only a single observation of the $[(3x1) + \sqrt{3}]$ domain and no observations of the $[(1 \times 1) + \sqrt{3}]$ domain. Note, however, that our observations would move the upper boundaries of the $[(1 \times 1) + \sqrt{3}]$ and $[(3x1) + \sqrt{3}]$ regions to slightly higher temperatures.

Our LEEM and LEED measurements also confirm the region in Fig. 1 exclusively composed of Ag (3x1) and Ge at low Ag coverages. For deposition at 370 °C, we observed (3x1) growth before (4x4) growth (Fig. 2). However, the (4x4) phase formed at lower coverage (0.1ML) than the 0.2 ML predicted by Grozea et al. ¹² In contrast to their region of exclusively (3x1) from ~0.15-0.37 ML, with no Ge, we did not observe a surface composed entirely of (3x1) at any point during deposition on Ge(111) at either 370 °C or 410 °C.

IV. CONCLUSIONS

The (3x1) phase has received relatively less attention from prior Ag/Ge(111) studies. We observed the (3x1) phase at multiple locations in the Ag/Ge(111) phase diagram, whereas most previous studies had only reported (3x1) as growing in small insets between (4x4) Ag or Ge(111) c(2x8), an observation that corresponds with our STM and LEED measurements shown in Fig. 3. The coexistence of (3x1) with (4x4) and/or $\sqrt{3}$ phases was observed with LEED at multiple coverages and temperatures (Figs. 5, 6, 7). LEEM and LEED images also showed that (3x1) is the only Ag phase on the surface from 0.05-0.1 ML at 370 °C deposition (Fig. 2(ab)). Detailed comparisons of our observations with the phase diagram in Fig. 1 were given in Sect. III.D. Our

observations confirmed the [(1 x 1) + $\sqrt{3}$] region at high temperature (>480 °C) for coverages greater than ~0.4 ML that had been missing experimental verification (Fig. 1). A significant difference from the phase diagram in Fig. 1 is that the equilibrium phase at low temperatures (<350°C) for coverages less than 0.38 ML is a mixture of (3x1) and (4x4), as opposed to (4x4) alone. Future calculations may be able to explain the energetics that control the formation of these different phases.

DEDICATION

This paper is dedicated to Professor Charles S. Fadley, who was a brilliant experimental surface scientist and extraordinary educator, mentor, and colleague. His long friendship and collegiality, plus helpful scientific and career advice, with the senior author (SC) over more than 30 years are gratefully acknowledged. The first author (CHM) also wishes to acknowledge Prof. Fadley for knowledge imparted through his graduate surface physics course and his guidance as member of qualifying examination and dissertation committees.

ACKNOWLEDGMENTS

We acknowledge partial funding support for this work from the National Science Foundation under grants PHY-0649297 (ALR), CHE-0719504, and DMR-1710748. We also thank Eric Poppenheimer for writing the software that was used to display and analyze the LEEM and LEED data files.

DATA AVAILABILITY

The data that support the findings of this study are available from the corresponding author upon reasonable request.

REFERENCES

- ¹M. Bertucci, G. Lelay, M. Manneville, and R. Kern, Surface Science **85**, 471 (1979).
- ²M. Hammar, M. Gothelid, U. O. Karlsson, and S. A. Flodstrom, Phys. Rev. B 47, 15669 (1993).
- ³H. Huang, H. Over, S. Y. Tong, J. Quinn, and F. Jona, Phys. Rev. B **49**, 13483 (1994).
- ⁴T. Takahashi and S. Nakatani, Surface Science **282**, 17 (1993).
- ⁵G. Lelay, et al., Surface Science **309**, 280 (1994).
- ⁶G. Lelay, Surface Science **132**, 169 (1983).
- ⁷G. Lelay, G. Quentel, J. P. Faurie, and A. Masson, Thin Solid Films **35**, 273 (1976).
- ⁸G. Lelay, G. Quentel, J. P. Faurie, and A. Masson, Thin Solid Films **35**, 289 (1976).
- ⁹P. B. Howes, C. Norris, M. S. Finney, E. Vlieg, and R. G. Vansilfhout, Physical Review B **48**, 1632 (1993).
- ¹⁰L. Seehofer and R. L. Johnson, Surface Science **318**, 21 (1994).
- ¹¹R. Plass and L. D. Marks, Surface Science **380**, 497 (1997).
- ¹²D. Grozea, E. Bengu, and L. D. Marks, Surface Science **461**, 23 (2000).
- ¹³D. Grozea, E. Bengu, C. Collazo-Davila, and L. D. Marks, Surface Review and Letters **6**, 1061 (1999).
- ¹⁴D. J. Spence and S. P. Tear, Surface Science **398**, 91 (1998).
- ¹⁵M. Padovani, E. Magnano, G. Bertoni, V. Spreafico, L. Gavioli, and M. Sancrotti, Applied Surface Science **212**, 213 (2003).
- ¹⁶H. M. Zhang and R. I. G. Uhrberg, Appl. Surf. Sci. **212**, 353 (2003).
- ¹⁷M. Gothelid, M. Hammar, U. O. Karlsson, C. Wigren, and G. Lelay, Phys. Rev. B **52**, 14104 (1995).
- ¹⁸R. J. Phaneuf and M. B. Webb, Surface Science **164**, 167 (1985).
- ¹⁹C. Collazo-Davila, et al., Surface Science **418**, 395 (1998).
- ²⁰Y. G. Ding, C. T. Chan, and K. M. Ho, Phys. Rev. Lett. **67**, 1454 (1991).
- ²¹D. Grozea, E. Bengu, C. Collazo-Davila, and L. D. Marks, Surface Review and Letters **6**, 1061 (1999).
- ²²C. Collazo-Davila, D. Grozea, and L. D. Marks, Physical Review Letters **80**, 1678 (1998).
- ²³H. H. Weitering and J. M. Carpinelli, Surface Science **384**, 240 (1997).
- ²⁴J. A. Giacomo, Ph.D. dissertation in Physics, University of California, (2009).
- ²⁵C. L. H. Devlin, D. N. Futaba, A. Loui, J. D. Shine, and S. Chiang, Mat. Sci. Engin. B. **96**, 215 (2002).
- ²⁶C. H. Mullet and S. Chiang, Journal of Vacuum Science & Technology A 31, 020602 (2013).

Figure Captions

Fig. 1. Ag/Ge(111) surface phase diagram proposed by Grozea et al. in Ref. 12. Reprinted from Surface Science, Vol. 461, D. Grozea, E. Bengu, and L. D. Marks, Surface phase diagrams for the Ag–Ge(111) and Au–Si(111) systems, pages 23-30, Copyright (2000), with permission of Elsevier.

Fig. 2. LEED patterns and LEEM images before and after desorption of Ag (3x1) from Ge(111). (a) After deposition of 0.05-0.1 ML Ag at 370 °C. Ag (3x1) LEED spots (dashed arrow) coexist with Ge (2x1) LEED features (diamond head arrow), which were present before the Ag deposition. (b) After Ag deposition on Ge(111), LEEM image corresponding to the (3x1) LEED pattern in (a). Ge (dark areas) and Ag (3x1) (bright areas). FOV 5 μm. (c) Clean Ge (2x1) LEED pattern after desorption of Ag. (d) LEEM image corresponding to LEED pattern in (c), after desorption of Ag. FOV 5 μm.

Fig 3. (color online) Ag deposited on Ge(111) at 330 °C while imaging with LEEM and LEED, followed by STM measurements at room temperature. $\Theta = 0.59$ ML. (a) LEED picture showing $\sqrt{3}$, (4x4), and faint (3x1) spots. Several spots are indicated with arrows: $\sqrt{3}$ (dotted arrow), (3x1) (dashed arrow), and the $[0, \frac{1}{2}]$ (4x4) spot (dot-dash arrow). (b) LEEM image showing regions with $\sqrt{3}$ (bright) and (4x4) (dark) structures. FOV = 2 μ m, E = 4.0 eV. E = 8.1 eV. (c) Empty state STM image. Regions of (4x4), c(2x8), and (3x1) Ag indicated. Sample bias = +1.0 V, tunneling current = 0.5 nA. 19 nm x 15 nm.

Fig. 4. LEED patterns and LEEM images of the deposition of 0.3 ML Ag onto Ge(111) at 170 °C. Diamond head arrows and dotted arrows point to the Ge(2 x 1) and \Box 3 Ag LEED spots, respectively. Solid arrows point to first-order Ge(111) LEED spots. (a) Clean Ge(111) LEED image. First order LEED spots (solid arrow) as well as Ge(2x1) features (diamond head arrow) are visible at this energy. (b) Clean Ge(111) LEEM image. 5 \Box m FOV. The sample surface has a high step density, especially on the periphery of the field of view. Small dark circles are defects in the microchannel plate, and larger dark spots are substrate defects. (c) LEED image shows additional $\sqrt{3}$ Ag spots (dotted arrow) after deposition of 0.3 ML Ag. (d) LEEM image corresponding to LEED image in (c), after deposition of 0.3 ML Ag. Dark areas correspond to $\sqrt{3}$ Ag and bright areas to Ge regions. 5 \Box m FOV.

Fig. 5. After dosing 0.3ML Ag on Ge(111), LEED images during heating to indicated temperatures. See Fig. 4 for LEED/LEEM of this sample after initial deposition. Different arrows in (b) identify LEED spots: Ge(2 x 1) (diamond head arrow), Ag (3x1) (dashed arrow), Ag (4x4) (dot-dash arrow), and Ag \Box 3 (dotted arrow). (a) $\sqrt{3}$ Ag

and (2×1) Ge. (b) Four coexisting structures are evident: $\sqrt{3}$ Ag, (2×1) Ge, (3×1) Ag, and (4×4) Ag (faint). (c) Spot intensities have changed for the 4 coexisting structures: $\sqrt{3}$ Ag, (2×1) Ge (faint), (3×1) Ag, (4×4) Ag. (d) Only (3×1) Ag and (4×4) Ag spots remain.

Fig. 6. Upon cooling the sample shown in Fig. 5(d), the LEED pattern does not change significantly. The Ag \Box 3 phase does not return after cooling. (a) 4 \Box m LEEM images of Ge(111) (bright areas) covered with small (\leq 100 nm) domains of [(4x4) + (3x1)] (dark areas). It is not possible to distinguish between the (4x4) and (3x1) phases. The largest dark spots in the image are substrate defects. (b) LEED pattern of the surface in (a), showing (4x4) (dotdash arrow) and (3x1) (dashed arrow) spots.

Fig. 7. Heating 0.5 ML Ag in LEED. Arrows identify LEED spots: Ge (1 x 1), solid arrow; Ag \Box 3, dotted arrow; Ag (3x1), dashed arrow; Ag (4x4), dot-dash arrow. (a) After deposition of 0.5 ML Ag at 220 °C, $\sqrt{3}$ Ag. (b) $\sqrt{3}$ Ag + (4x4) Ag + (3x1) Ag (faint). (c) $\sqrt{3}$ Ag + (3x1) Ag (very faint). (d) $\sqrt{3}$ Ag + (3x1) Ag (very faint). (e) Clean Ge after Ag desorption.